

# Tin(IV) porphyrin functionalization of electrochemically active fluoride-doped tin-oxide (FTO) via Huisgen [3+2] click chemistry

Shiva Prasad<sup>a</sup>, Mohan Bhadbhade<sup>b</sup> and Pall Thordarson<sup>\*a</sup>◇

<sup>a</sup> School of Chemistry, The University of New South Wales, Sydney, NSW 2052, Australia

<sup>b</sup> Analytical Centre, The University of New South Wales, Sydney, NSW 2052, Australia

Received 5 November 2010

Accepted 15 January 2011

**ABSTRACT:** A novel tetra-alkyne terminated tin(IV) porphyrin **3** was synthesized in good yields and characterized using NMR spectroscopy, high resolution mass spectrometry and X-ray crystallography, the latter revealing interactions with hexane molecules that stabilize the crystal structure of the tin(IV) porphyrin **3**. It was then linked to a conductive fluorine-doped tin oxide (FTO) surfaces using Huisgen [3+2] click chemistry. The attachment of the tin(IV) porphyrin to the FTO surface **6** was characterized by X-ray photoelectron spectroscopy (XPS), indicating the presence of the 1,2,3-triazole unit. Electrochemical measurements of the tin(IV) porphyrin modified FTO surface **7** show that it is still electrochemically active with oxidation ( $E_{pa}$ ) and reduction peaks ( $E_{pc}$ ) for the ferricyanide redox couple observed at  $E_{pc}$  and  $E_{pa}$  of -0.144 and +0.568 V vs. Ag|AgCl respectively, representing a modest shift of ca. +/- 0.1–0.15 V, compared to unmodified FTO.

**KEYWORDS:** surface functionalization, tin(IV) porphyrin, XPS, FTO, electrochemistry.

## INTRODUCTION

Currently, there is an extensive amount of work focused on the study of photo-driven processes and devices, particularly in the field of renewable energy research in the form of solar cells [1–6]. Most of this effort is focused on searching for chromophores capable of efficiently generating photocurrent on appropriately designed electrodes. The ideal chromophores for this purpose requires a combination of unique electronic [7], photonic [8] and catalytic properties [9, 10]. One particular class of chromophores that has drawn a lot of interest are metalloporphyrins. Metalloporphyrins are long been known to act as good photosensitizers due to their long-lived excited states, good quantum yields of excitation and excellent visible light absorption and redox properties [11, 12]. Representative examples of frequently used metalloporphyrins as photosensitizers include zinc [13], tin [14],

nickel [15], rhodium [16] and iron [17] porphyrins. In particular, zinc(II) and tin(IV) metalloporphyrins are most commonly used as photosensitizers as they have most of the above properties for a good photocatalyst. This includes a number of recent demonstration of the use of zinc(II) porphyrins in dye-sensitized solar cells [18–20] and the application of tin(IV) porphyrins as photocatalyst to generate metallic nanostructures [21, 22].

To be useful in photo-driven devices such as light activated biosensors, biofuel cells and solar cells preferably requires the metalloporphyrin chromophores to be attached to transparent conductive electrodes. Recent studies show that electrodes functionalized with free-base porphyrin chromophores can generate photocurrent in the presence of light and a sacrificial electron donor. The free-base tetraphenyl porphyrin-fullerene dyad modified indium tin oxide (ITO) surface reported by Fukuzumi and coworkers showed up to 100 nA photocurrent in the presence of triethanolamine as an electron donor and an applied potential bias [23]. Similarly, Hirano and coworkers have been able to generate photocurrent with a mesoporous silica-porphyrin hybrid coated on a

◇SPP full member in good standing

\*Correspondence to: Pall Thordarson, email: p.thordarson@unsw.edu.au, tel: +61 2-9385-4478

fluorine-doped tin oxide (FTO) electrode [24]. When the system is exposed to a switching light source under a bias of -0.4 to 0.3 V, a photocurrent is detected.

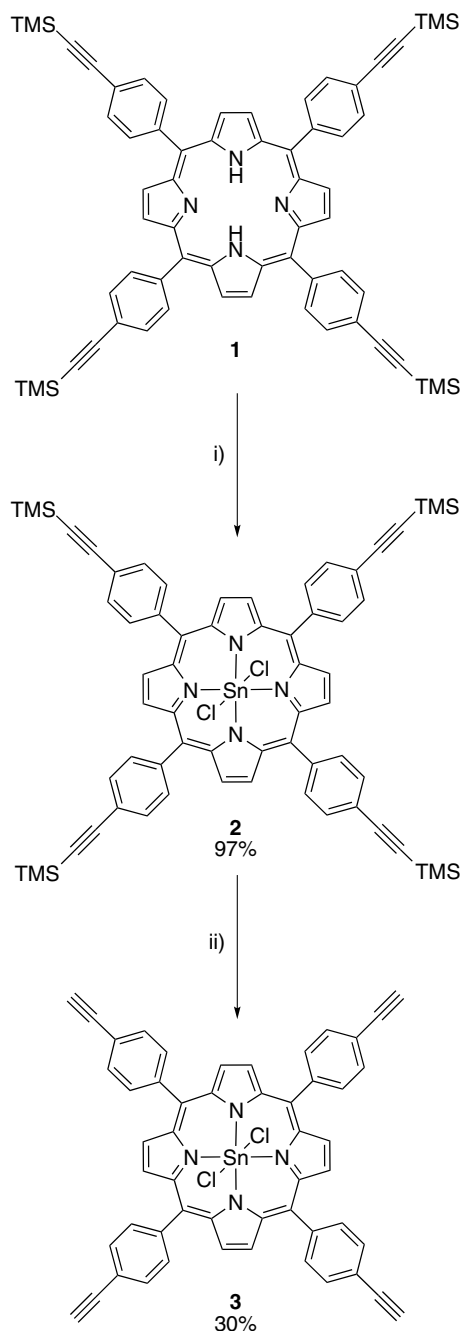
Here we describe the synthesis of novel tin(IV) porphyrin that has been linked to a FTO surface using the Huisgen [3+2] click reaction. The resulting tin(IV) porphyrin modified FTO surface were characterized by X-ray photoelectron spectroscopy (XPS) and shown to be electrochemically active. This represents an effective and generic way to generate metalloporphyrin modified electrodes for use in photo-driven devices.

## RESULTS AND DISCUSSION

### Synthesis and characterization of tin(IV) porphyrins

The tin(IV) porphyrin **3** was obtained in three steps as shown in Scheme 1. The precursor trimethylsilane (TMS) protected free-base porphyrin **1** was synthesized in 37% yield following the method reported by McDonald and coworkers [25]. The subsequent metalation to afford dichlorotin(IV) porphyrin **2** was achieved using the Rothmund method [26] where **1** was refluxed with an excess of tin(II) chloride to afford **2** in 97% yield. The TMS-groups were then removed to afford the target tetra-alkyne tin(IV) porphyrin **3** in 30% yield by refluxing potassium carbonate with tin(IV) porphyrin **2** in a dichloromethane/methanol mixture (Scheme 1) [27].

In each step of this synthesis, the porphyrins were isolated in good purity by precipitation or by washing the organo-soluble porphyrins (**1–3**) with water. The structure of these compounds was determined by a combination of spectroscopic techniques, including  $^1\text{H}$  and high resolution mass spectrometry. The UV-vis (Fig. 1a) and  $^1\text{H}$  NMR spectra for **2** (Fig. 1b) and **3** (Fig. 1c) are similar to previously reported tin(IV) porphyrins [28]. Following the metalation,  $^1\text{H}$  NMR the -2.83 ppm resonance for the inner pyrrolic N-H in **1** disappeared and the insertion of the tin metal was confirmed by MS (1000.53  $m/z$ ) and UV-vis with a Soret band at 430 nm and two Q-bands at 602 and 561 nm, respectively. After removal of the TMS-group to form **3**, the coupling constant of the  $^{119}\text{Sn}$  NMR (-590.08) suggested that the axial ligands were chlorides [28]. This was somewhat unexpected as the conditions used for converting **2** and **3** have been reported to result in ligand exchange from a chloride to a hydroxide. It is possible that chloroform, which was used as a solvent for recrystallization, could have degraded to form phosgene and hydrochloric acid. The resulting chlorides from hydrochloric acid could then exchange with the labile hydroxyl ligands, accounting for the observed chlorides in **3**. Signs of **3** converted to the dihydroxy ligated species did show in MALDI-TOF mass spectrometry analysis but this ligand exchange may have happened during sample preparation or *in situ* in the mass spectrometer.



**Scheme 1.** Reagents and conditions: (i) tin(II) dichloride, pyridine, reflux, overnight; (ii) potassium carbonate, methanol:dichloromethane (1:4), reflux, 16 h

Single crystals of tin(IV) porphyrin **3** were grown for X-ray crystallography by slow diffusion of hexane into a solution of **3** in chloroform. Due to the small crystal size, acquisition of data for X-ray crystallographic analysis was carried out at the synchrotron X-ray source at the Australian Synchrotron Centre. The data was collected with 10223 reflections with an R factor of 0.1143. The quality of the data obtained was sufficient to confirm the main structural features of the tin(IV) porphyrin **3**, including the nature of the axial ligands as chlorides.

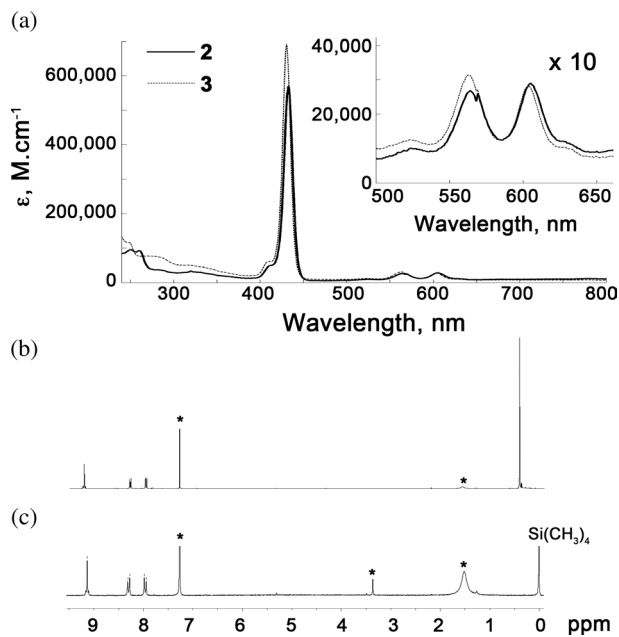


**Fig. 1.** Spectra of **2** and **3**; (a) UV-vis spectra ( $\text{CHCl}_3$ ) of **2** and **3**.  $^1\text{H}$  NMR (300 MHz,  $\text{CDCl}_3$ ) of (b) **2** and (c) **3** (solvent impurities are labeled with \*)

As illustrated in Fig. 2a, the tin metal ion sits expectedly within the porphyrin macrocycle with a N-Sn-N bond angle of  $180^\circ$  and a N-Sn bond length of  $2.1 \text{ \AA}$ . The Cl-Sn-N bond angle, which is expected to be approximately  $90^\circ$ , was observed to be  $87^\circ$ . This is because the axial chloride ligand sits next to the hexane molecule. Moreover, the *meso*-porphyrin phenyl rings of the tin(IV) porphyrin **3** are rotated approximately  $79^\circ$  to the plane of the porphyrin macrocycle. The tin(IV) porphyrin macrocycles pack in a unique way, where one macrocycle is approximately  $40^\circ$  to the following tin(IV) porphyrin macrocycle (Fig. 2b). The three-dimensional packing of tin(IV) porphyrin **3** is shown in Fig. 3.

The porphyrin packs into a crystal lattice in the presence of hexane that was used during the growth of these

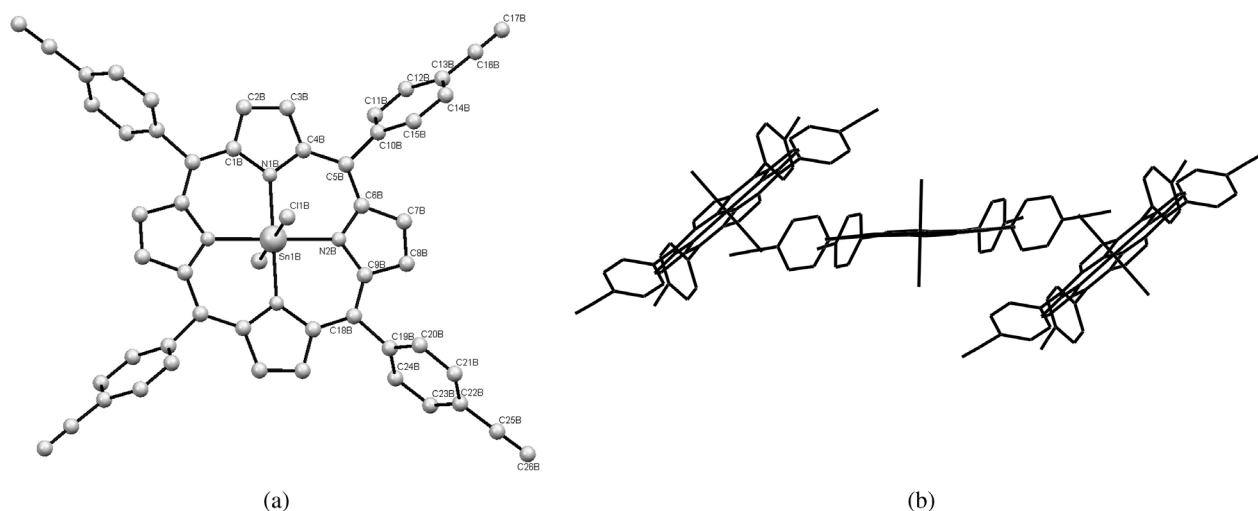


**Fig. 2.** X-ray crystallographic analysis of tin(IV) porphyrin **3**. (a) Front view and (b) the unique packing of tin(IV) porphyrin **3** along the crystallographic b-axis. The hydrogen atoms are excluded for clarity

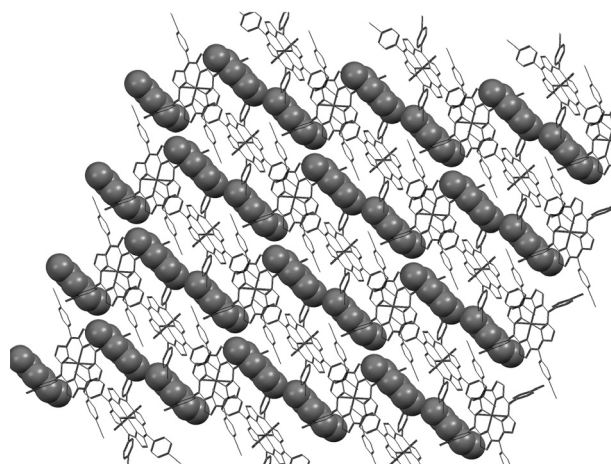
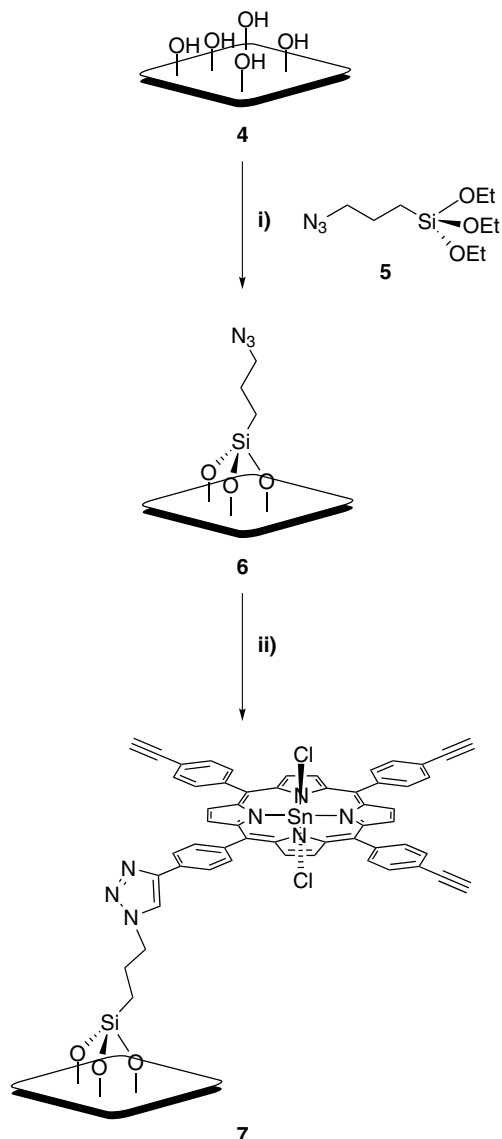


**Fig. 3.** A perspective view of the tin(IV) porphyrin **3** along the crystallographic a-axis. The hydrogen atoms are excluded for clarity. The packing of tin(IV) porphyrin **3** (wireframe) is shown in the presence of hexane (spacefill)

crystals. These hexane molecules are important for the stability of the crystal lattice of tin(IV) porphyrin **3**. Along the crystallographic a-axis, these porphyrin molecules pack as close to each other as possible, with the hexane molecules sitting in between each porphyrin. The axial chlorides of the porphyrin interacts with the hydrogen of the C3-hexane molecules, while the phenyl ring of an adjacent porphyrin molecule interacts with the same hexane, however at the C1-position, causing the alkene group ( $\text{C}\alpha\text{C}-\text{C}$ ) to be slightly kinked ( $178^\circ$ ). Along the crystallographic b-axis, each tin(IV) porphyrin macrocycle sits approximately  $40^\circ$  to the following tin(IV) porphyrin, creating a unique form of packing.

### Synthesis and characterization of tin(IV) porphyrin-modified FTO surfaces

The tin(IV) porphyrin modified surface **7** was prepared using the copper(I) catalyzed Huisgen [3+2] click



**Scheme 2.** (Left) the attachment of tin(IV) porphyrin **3** to the azide-modified FTO surface **6**; (i) (3-azidopropyl)triethoxysilane **5** (40 mM), toluene, 2 h, room temperature; (ii) tin(IV) porphyrin **3**, copper(II) sulfate, ascorbic acid, *N,N*-dimethylformamide, water, overnight (the presence of chloride axial ligands are assumed but cannot be verified by XPS or UV-vis spectroscopy)

chemistry approach [29] outlined in Scheme 2. The (3-azidopropyl)triethoxysilane **5** precursor was initially synthesized in 95% yields using methods adopted from Khoukhi and coworkers [30]. The azide linker **5** was added to the activated FTO surface **4** in a solution of toluene (Scheme 2). The resulting azide-modified FTO surface **6** was washed and sonicated in dichloromethane, chloroform, methanol and acetone to clean the surface of any absorbed compounds. The tetra-alkyne terminated tin(IV) porphyrin **3** was then attached to surface **6** using the copper(I) catalyzed Huisgen [3+2] click chemistry method adopted from Ortega-Munoz [31]. The azide-modified FTO surface **6** was reacted with a catalytic

amount of copper(II) sulfate, ascorbic acid and tin(IV) porphyrin **3** in *N,N*-dimethylformamide and water to yield the tin(IV) porphyrin triazole-modified FTO surface **7**. Scheme 2 outlines a step-wise modification of tin(IV) porphyrin to FTO surfaces.

The tin(IV) porphyrin-modified FTO surface **7** was analyzed using XPS (Fig. 4a,b) and surface reflectance UV-vis spectroscopy (Fig. 4c). The N1s XPS spectra of the azide-modified FTO surface **6** (Fig. 4a) show two distinct peaks at 404.7 eV and 400.6 eV in a 1:2 ratio which correspond to the center electron deficient azide nitrogen and the two nearly equivalent terminal azide nitrogen atoms as previously reported in the literature [32]. Following the Huisgen [3+2] click chemistry reaction to form the tin(IV) porphyrin triazole-modified FTO surface **7**, the 404.7 eV peak disappears (Fig. 4b), leaving one peak at 400.4 eV for the near-equivalent 1,2,3-triazole nitrogens, indicating that the reaction of the azide with the terminal alkyne of tin(IV) porphyrin **3** to a 1,2,3-triazole was successful and therefore effectively linking the tin(IV) porphyrin **3** to the surface [32]. In addition, surface reflectance UV-vis spectral data (Fig. 4c) shows the characteristic Soret peak of the tin(IV) porphyrin chromophore at 432 nm following the attachment of tin(IV)

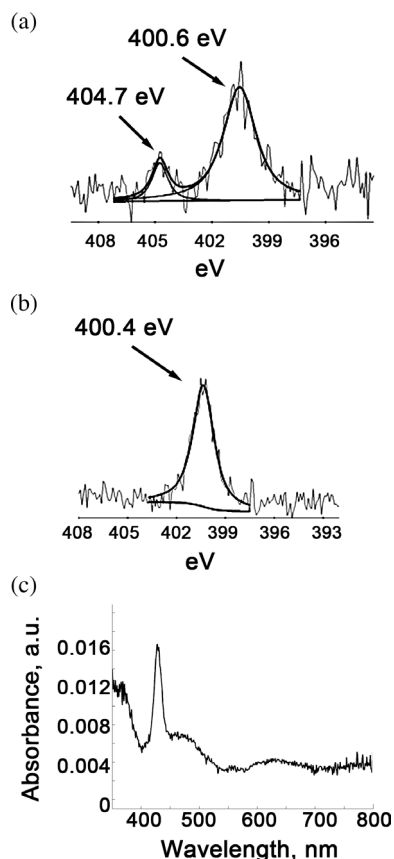


**Fig. 4.** Characterization spectra for FTO modified surfaces; the N1s XPS spectra of FTO modified surfaces (a) **6** and (b) **7**. (c) The UV-vis reflectance of FTO modified surface **7** showing the porphyrin peak at 432 nm (absorption below  $\approx$  380 nm is due to the glass in FTO)

porphyrin **3** to the azide-modified FTO surface **6**. It should be noted that surface reflectance UV-vis spectroscopy does not distinguish between covalently attached ligands or surface absorbed molecules. However, the absorbance spectrum observed for the tin(IV) porphyrin triazole-modified FTO surface **7** did not change even after continuous sonication to remove adhered contaminants in solvents such as dichloromethane, chloroform, toluene, acetone, methanol and *N,N*-dimethylformamide.

### Electrochemical characteristics of surface **7**

Cyclic voltammetry (CV) measurements of the tin(IV) porphyrin-modified FTO electrodes were performed in an effort to gain information about the electroactivity of the modified FTO surfaces, using a ferricyanide probe.

Previous electrochemical studies of tin(IV) porphyrins suggest that the first reduction of tin(IV) porphyrins occurs at about  $-0.7$  V vs. SCE [33, 34]. However, this falls outside the linear current region of unmodified FTO surfaces, as reduction of tin in FTO surfaces occurs at approximately  $-0.5$  to  $-0.6$  V vs. Ag|AgCl (Fig. 5, thin black line). For this reason, the reduction peak of tin(IV) porphyrin-modified on FTO surfaces was not observed directly. In order to obtain information about the porphyrin layers, ferricyanide ( $\text{Fe}(\text{CN})_6^{3+}$ ) was used as a probe to measure the changes in response during each modification step. The cyclic voltammogram ( $-0.4$  to  $1.0$  V vs. Ag|AgCl) for each modification step leading up to the synthesis of tin(IV) porphyrin triazole-modified FTO surface **7**, using ferricyanide as a redox probe, is shown in Fig. 4. The activated FTO surface **4** (Fig. 5, thin gray line) shows large reversible ferricyanide with oxidation ( $E_{\text{pa}}$ ) and reduction peaks ( $E_{\text{pc}}$ ) at  $+0.441$  V vs. Ag|AgCl

and  $+0.006$  V vs. Ag|AgCl respectively, consistent with an accessible electrode surface. After modification, this response decreases, consistent with a surface blocking layer. The azide-modified FTO surface **6** (Fig. 5, thick gray line) has an  $E_{\text{pc}}$  at  $+0.084$  V vs. Ag|AgCl and an  $E_{\text{pa}}$  at  $+0.384$  V vs. Ag|AgCl. Following the attachment of the tin(IV) porphyrin **3** chromophore, peaks with  $E_{\text{pc}}$  and  $E_{\text{pa}}$  of  $-0.144$  and  $+0.568$  V vs. Ag|AgCl were detected on the tin(IV) porphyrin triazole-modified FTO surface **7** respectively (Fig. 5, thick black line). The change in  $E_{\text{pc}}$  and  $E_{\text{pa}}$  are attributed to the increased distance from the FTO surface to the terminal tin(IV) porphyrin chromophores. As the length of the monolayer increases from surface **6** to **7**, the rate of electron transfer from the redox probe to the surface decreases, resulting in an increase in  $\Delta E$ . The ratio of the area under the reduction and oxidation peaks for surfaces **6** and **7** ( $i_{\text{pa}}/i_{\text{pc}}$ ) was calculated to be approximately 1, indicating the redox processes are reversible and stable under the working conditions ( $0.05$ – $0.60$  V/s). The tin(IV) porphyrin triazole-modified FTO surface **7** also shows a reduction in current when compared to the azide-modified precursor FTO surface **6**. The azide-modified FTO surface **6** has a cathodic peak current ( $i_{\text{pc}}$ ) and an anodic peak current ( $i_{\text{pa}}$ ) of  $-77$  and  $+51$   $\mu\text{A}$  respectively, whilst the tin(IV) porphyrin triazole-modified FTO surface **7** has an  $i_{\text{pc}}$  and  $i_{\text{pa}}$  of  $-51$  and  $+25$   $\mu\text{A}$ .

## EXPERIMENTAL

### Chemicals and instruments

All chemicals were purchased from Sigma Aldrich with the exception of propionic acid, potassium carbonate, pyridine, anhydrous sodium sulfate (Ajax Finchem Pty. Ltd.) and tin(II) chloride dihydrate (Merck). Solvents were used as is from the manufacturers. Dichloromethane and methanol were distilled before use or obtained from Pure Solv dry solvent system (Innovative Technology Inc. #PS-MD-7). Pyrrole was purchased from Merck and freshly distilled or purified over aluminum oxide before use. The  $^1\text{H}$  Nuclear Magnetic Resonance ( $^1\text{H}$  NMR) spectra were recorded on a Bruker Avance DPX 200 Bruker Avance DPX 300 or on an Avance III 400 MHz spectrometers at 300 K. Signals were reported in ppm relative to tetramethylsilane ( $\text{SiMe}_4$ , ( $^1\text{H}$ ) = 0). The  $^{119}\text{Sn}$  NMR spectra were obtained on a Bruker Avance III 400 MHz spectrometer as stated, quoted in ppm relative to tetramethyltin ( $\text{Sn}(\text{CH}_3)_4$ ,  $^{119}\text{Sn}$  = 0 ppm) as an external standard. Infra-red (IR) spectroscopy was recorded on a Thermo Nicolet Avatar model 370 FT-IR spectrometer or on a Shimadzu FTIR-8400S by solid state. UV-vis spectra were recorded either on a Varian Cary 5E UV-vis-NIR or a Varian Cary 50Bio UV-visible spectrophotometer. Electrospray ionisation (ESI) mass spectra were recorded on a ThermoQuest Finnigan LCQ-DECA electrospray instrument equipped with a Xcaliber processing software

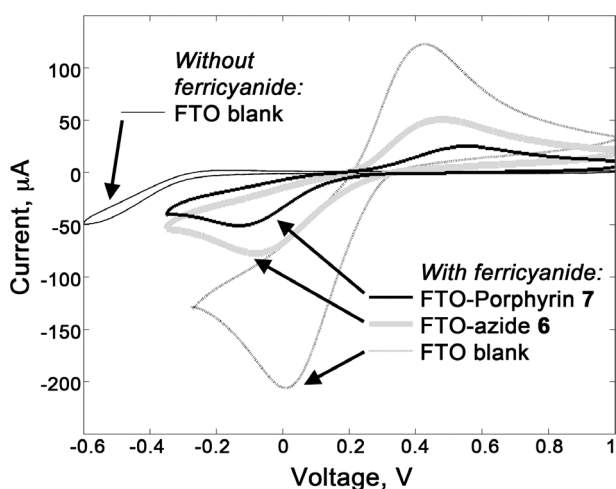


**Fig. 5.** Cyclic voltammograms for the bare activated FTO surface **4**, FTO with ferricyanide, the azide-modified FTO surface **6** and the tin(IV) porphyrin triazole-modified FTO surface **7**. These results were obtained using ferricyanide (1 mM) and potassium chloride (200 mM) as supporting electrolyte in phosphate buffer (100 mM, pH 7.0) with platinum counter and Ag|AgCl reference electrodes at a scan rate of 0.1 mV/s

or on a Waters Micromass ZQ 2000 ESCi equipped with MassLynx version 4.1. Matrix assisted laser desorption ionisation (MALDI) was performed on a Applied Biosystems Voyager DE STR MALDI (reflectron mode) with the matrix trans-2-[3-(4-*tert*-butylphenyl)-2-methyl-2-propenylidene]-malononitrile. High resolution ESI (HR-MS) mass spectrometry was performed on a Thermo Linear Quadrupole Ion Trap Fourier Transform Ion Cyclotron Resonance (LQT FT Ultra) mass spectrometer in electrospray mode with a 7 T superconducting magnet at the BMSF, Analytical Centre at the University of New South Wales. Melting points were recorded using a Mel-Temp II melting point apparatus and are uncorrected. standard. Cyclic Voltammetry was performed on either a Electrochemical Analyzer BAS100B (BASi) utilizing BAS100W software or on a Autolab Potentiostat PGSTAT 12 equipped with GPES version 4.9. Surface modified electrodes were analyzed in a solution of 100 mM phosphate buffer (pH 7.0) with 200 mM potassium chloride and 1 mM ferrocyanide with Ag|AgCl reference and platinum counter electrodes. Each sample was deoxygenated by bubbling dry nitrogen for 5 min prior to electrochemical analysis. X-ray Crystallography work in this research was undertaken on the macromolecular crystallography beamline at the Australian Synchrotron, Victoria, Australia. Surface analysis by X-ray photoelectron spectroscopy (XPS) was performed on a VG ESCALAB 220-IXL imaging XPS microscope with an Al K $\alpha$  X-ray (1486.6 eV) anode source. Surface UV-vis absorption measurements were made using a Cary 5 UV-vis-NIR fitted with a diffuse reflectance apparatus. The 5,10,15,20-tetrakis[(4-trimethylsilyl)ethynyl-phenyl]porphyrin **1** was synthesized according to literature procedure [25]. UV-vis (CH<sub>2</sub>Cl<sub>2</sub>):  $\lambda_{\max}$ , nm (log  $\epsilon$ ) 422 (5.65), 516 (4.38), 551 (4.18), 589 (3.88), 645 (3.86). <sup>1</sup>H NMR (200 MHz, CDCl<sub>3</sub>, Me<sub>4</sub>Si):  $\delta_{\text{H}}$ , ppm -2.83 (2H, s, pyrrole-NH), 0.38 (36H, s, Si(CH<sub>3</sub>)<sub>3</sub>), 7.79 and 8.16 (16H, ABq,  $J = 9.0$  Hz, Ph), 8.81 (8H, s, pyrrole-H). FTIR (KBr):  $\nu$ , cm<sup>-1</sup> 3313 (w), 2956 (m), 2156 (s), 1497 (s), 1474 (s), 1249 (s), 966 (s), 869 (s). MS (ESI):  $m/z$  1000.53 (calcd. for [M + H]<sup>+</sup> 999.55).

**Dichloro[5,10,15,20-tetrakis((4-trimethylsilyl)ethynylphenyl)porphyrinato] tin(IV) (2).** The 5,10,15,20-tetrakis[(4-trimethylsilyl)ethynylphenyl]porphyrin **1** (300 mg, 300  $\mu\text{mol}$ ) was dissolved in pyridine (100 mL) and heated to reflux. Tin(II) chloride dihydrate (270 mg, 1.20 mmol) was added and the solution was allowed to reflux in air for 12 h in the absence of light. After cooling, dichloromethane was evaporated and water (150 mL) was added. The aqueous layer was then extracted with dichloromethane (3  $\times$  100 mL). The combined organic extracts were then washed with water (3  $\times$  100 mL) and aqueous hydrochloric acid (1 M, 2  $\times$  100 mL). The organic layers were combined, dried over anhydrous sodium sulfate and filtered. The dichloro[5,10,15,20-tetrakis((4-trimethylsilyl)ethynylphenyl)porphyrinato]-tin(IV) porphyrin **2** was collected under reduced pressure

as fine purple crystals (347 mg, 97%), mp > 300 °C. UV-vis (CH<sub>2</sub>Cl<sub>2</sub>):  $\lambda_{\max}$ , nm (log  $\epsilon$ ) 431 (5.74), 562 (4.29), 603 (4.27). <sup>1</sup>H NMR (300 MHz, CDCl<sub>3</sub>, Me<sub>4</sub>Si):  $\delta_{\text{H}}$ , ppm 0.39 (36H, s, Si(CH<sub>3</sub>)<sub>3</sub>), 7.93 and 8.25 (16H, ABq,  $J = 8.2$  Hz, Ph), 9.19 (8H, s, satellites, <sup>4</sup> $J_{\text{H-Sn}} = 14.8$  Hz, pyrrole-H). <sup>119</sup>Sn NMR (149 MHz, CDCl<sub>3</sub>, Me<sub>4</sub>Sn):  $\delta_{\text{Sn}}$ , ppm -590.08 (Sn). FTIR (KBr):  $\nu$ , cm<sup>-1</sup> 2956 (m), 2898 (w), 2157 (s), 1499 (m), 1249 (s), 1030 (s), 864 (s). MS (MALDI):  $m/z$  1116.26 (calcd. for [M - 2Cl]<sup>+</sup> 1116.29). HR-MS (FT-ESI):  $m/z$  1147.3091 (calcd. for C<sub>65</sub>H<sub>63</sub>N<sub>4</sub>OSi<sub>4</sub>Sn: [M - 2Cl + OCH<sub>3</sub>]<sup>+</sup> 1147.2836), 1133.2935 (calcd. for C<sub>64</sub>H<sub>61</sub>N<sub>4</sub>OSi<sub>4</sub>Sn: [M - 2Cl + OH]<sup>+</sup> 1133.2958).

**Dichloro[5,10,15,20-tetrakis(4-ethynylphenyl)porphyrinato]tin(IV) (3).** The dichloro[5,10,15,20-tetrakis((4-trimethylsilyl)ethynylphenyl)porphyrinato]tin(IV) porphyrin **2** (84.3 mg, 71.0  $\mu\text{mol}$ ) was dissolved in dichloromethane (40 mL). To this was added a solution of potassium carbonate (1.10 g, 7.97 mmol) in methanol (10 mL) and the mixture was refluxed for 16 h in the absence of light. After cooling, the solvents were removed under reduced pressure and the crude solid was redissolved in dichloromethane (200 mL). The solution was washed with water (3  $\times$  100 mL) and the organic layer dried over anhydrous sodium sulfate. The final product was recovered by filtration and solvent removed under reduced pressure to give the dichloro[5,10,15,20-tetrakis(4-ethynylphenyl)porphyrinato]tin(IV) porphyrin **3** as a purple crystalline solid (22.1 mg, 29%), mp > 300 °C. UV-vis (CH<sub>2</sub>Cl<sub>2</sub>):  $\lambda_{\max}$ , nm (log  $\epsilon$ ) 430 (5.84), 561 (4.37), 602 (4.29). <sup>1</sup>H NMR (300 MHz, CDCl<sub>3</sub>, Me<sub>4</sub>Si):  $\delta_{\text{H}}$ , ppm 3.37 (4H, s, C $\equiv$ CH), 7.97 and 8.29 (ABq, 16H,  $J = 8.2$  Hz, Ph), 9.21 (8H, s, satellites, <sup>4</sup> $J_{\text{H-Sn}} = 14.8$  Hz, pyrrole-H). <sup>119</sup>Sn NMR (149 MHz, CDCl<sub>3</sub>, Me<sub>4</sub>Sn):  $\delta_{\text{Sn}}$ , ppm -588.77 (Sn). FTIR (KBr):  $\nu$ , cm<sup>-1</sup> 3289 (m), 2107 (w), 1498 (m), 1234 (s), 1029 (s), 856 (s), 813 (s). MS (MALDI):  $m/z$  861.72 (calcd. for [M - 2Cl + 2OH]<sup>+</sup> 861.53), 828.15 (calcd. for [M - 2Cl]<sup>+</sup> 828.13). HR-MS (FT-ESI):  $m/z$  859.1528 (calcd. for C<sub>53</sub>H<sub>31</sub>N<sub>4</sub>OSn [M - 2Cl + OCH<sub>3</sub>]<sup>+</sup> 859.1532).

**Activating FTO surface electrodes [38].** The FTO slides were washed by sonicating in acetone for 5 min followed by isopropanol for 5 min. The resulting slides were treated with a solution of H<sub>2</sub>O<sub>2</sub>:H<sub>2</sub>O (30%) and NH<sub>4</sub>OH:H<sub>2</sub>O (25%) at 80 °C for 20 min. The activated transparent slides were again rinsed with water and dried under nitrogen prior to use.

**(3-azidopropyl)triethoxysilane (5) [31, 39].** To a pre-heated solution (60 °C) of sodium azide (1.01 g, 15.5 mmol) in dimethyl sulfoxide was added (3-chloropropyl)triethoxysilane (2.00 g, 8.33 mmol) and stirred overnight. After cooling, water (100 mL) was added and the aqueous phase was extracted with diethyl ether (3  $\times$  100 mL), dried over anhydrous sodium sulfate and filtered. The (3-azidopropyl)triethoxysilane **5** was retrieved under reduced pressure as a clear yellow oil (1.96 g, 95%). <sup>1</sup>H NMR (CDCl<sub>3</sub>, 200 MHz):  $\delta$ , ppm 3.86–3.79 (m 2H, CH<sub>3</sub>CH<sub>2</sub>Si), 3.26 (t, 2H, N<sub>3</sub>CH<sub>2</sub>CH<sub>2</sub>,  $J = 7.1$  Hz),

1.74–1.68 (m, 2H,  $-\text{CH}_2\text{CH}_2\text{CH}_2$ ), 1.23 (t, 3H,  $\text{CH}_3\text{CH}_2\text{Si}$ ,  $J = 7.1$  Hz), 0.71–0.65 (m, 2H,  $\text{SiCH}_2\text{CH}_2$ ). These results were in good agreement with those found in literature [31].

**(3-azidopropyl)triethoxysilane-modified FTO (6).** To a pre-washed activated fluoride-doped tin oxide surface (ethanol then water, sonicated twice, each for 5 min) was added a solution of (3-azidopropyl)triethoxysilane **3** (98 mg, 396  $\mu\text{mol}$ ) in toluene (10 mL). The mixture was left to stand for 1.5 h and washed with toluene, then sonicated twice (5 min each) with toluene, ethanol and water. The resulting (3-azidopropyl)triethoxysilane-modified FTO surface **6** was then dried under nitrogen. XPS (orbital) eV: Si2p (102.29, OSiC), C1s (285.01 C-C) C1s (286.61, C-N), C1s (288.01, C-H<sub>x</sub>), N1s (400.73, N=N-N), N1s (404.74, N=N-N), O1s (531.01, O-C), O1s (532.14, O-Si), O1s (533.24, O-H). The XPS spectral data were in good agreement with those reported in literature [32].

**Dichloro[5,10,15,20-tetrakis(4-(ethynylphenyl)porphyrinato]tin(IV) porphyrin-modified FTO (7).** The (3-azidopropyl)triethoxysilane-modified FTO surface **6** was pre-washed in toluene, water, ethanol and acetone, then nitrogen dried prior to use. The FTO surface **6** was then sonicated in dry *N,N*-dimethylformamide. Separately, ascorbic acid (105 mg, 0.60 mmol) and copper(II) sulfate (100 mg, 626  $\mu\text{mol}$ ) were pre-dissolved in dry *N,N*-dimethylformamide (20 mL) and allowed to stir with **3** (35.9 mg, 41.6  $\mu\text{mol}$ ) for 15 min. The FTO surface **6** was then added and the deep purple mixture was allowed to stand overnight at room temperature in the absence of light. The surface was then washed with *N,N*-dimethylformamide, water, ethanol and acetone (sonicated, each for 5 min) and nitrogen dried to afford the tin(IV) porphyrin-modified FTO surface **7**. UV-vis surface reflectance spectroscopy: 432 nm; XPS (orbital) eV: C1s (285.06 C-C) C1s (286.55, C-N), C1s (288.23, C-H<sub>x</sub>), N1s (400.38, N-C), Sn3d5 (487.20, Sn-O), O1s (531.22, O-C), O1s (532.34, O-Si), O1s (533.47, O-H).

### X-ray structure determination

The X-ray diffraction measurement for **3** were carried out at the Australian Synchrotron Facility using graphite-monochromated synchrotron X-ray radiation ( $\lambda = 0.65253$  Å) at 120(2) K. The crystal, mounted on the goniometer using cryo loops for intensity measurements, was coated with paraffin oil and then quickly transferred to the cold stream using Oxford Cryo stream attachment. Symmetry related absorption corrections using the program XDS were applied and the data were corrected for Lorentz and polarization effects using the XDS software [36]. All structures were solved by Direct methods and the full-matrix least-squares refinements were carried out using SHELXL [37].

**Compound 3.**  $\text{C}_{52}\text{H}_{28}\text{Cl}_2\text{N}_4\text{Sn}$ . The data crystal had the form of a thin needle, dark red and had approximate dimension of  $0.11 \times 0.09 \times 0.02$  mm; triclinic, space group

*P-1*,  $a = 12.185(2)$  Å,  $b = 12.512(3)$  Å,  $c = 18.173(4)$  Å,  $\alpha = 71.95(3)^\circ$ ,  $\beta = 70.69(3)^\circ$ ,  $\gamma = 80.68(3)^\circ$ .  $Z = 2$ ,  $\rho_{\text{calcd}} = 1.260$  Mg/m<sup>3</sup>.  $\mu = 0.661$  mm<sup>-1</sup>.  $F(000) = 954.0$ . A total of 30,826 reflections were measured, 10,223 unique. The structure was refined on  $F^2$  to 0.1143, with R(F) equal to 0.2723 and a goodness of fit,  $S = 1.902$ .

### CONCLUSION

We were successful in the preparation and characterization of a novel alkyne-terminated tin(IV) porphyrin **3**, including obtain a crystal structure for **3**. We also described the successful synthesis of tin(IV) porphyrin modified FTO transparent electrode **7**. The tetra-alkyne terminated tin(IV) porphyrin **3** was attached to a transparent FTO electrode using Huisgen [3+2] click chemistry to link the porphyrin to the electrode *via* a 1,2,3-triazole structure. Electrochemical measurements of surface **7** using a ferricyanide probe show oxidation and reduction peaks at  $-0.144$  and  $+0.568$  V vs. Ag|AgCl, respectively. Following the successful attachment of tin(IV) porphyrin to the FTO surfaces described here, future studies will focus on the use of these electrodes in the photocatalytic generation of hydrogen which has been demonstrated by Shelnut and coworkers using tin(IV) porphyrin–platinum nanoaggregates [22, 35]. We are also currently exploring the use of these FTO surfaces for the regeneration of the oxidatively active biological markers such as the coenzyme NAD<sup>+</sup> and FAD but the reductive power of photoexcited tin(IV) porphyrins is well-placed to reduce these coenzymes [34].

### Acknowledgements

We thank the Australian Research Council for a discovery grant and an Australian Research Fellowship (DP0666325) to Pall Thordarson and the University of Sydney for a PhD scholarship to Shiva Prasad. We thank Dr. Tom Caradoc-Davies (Australian Synchrotron) for assistance. We would also like to thank Dr. Bill Bin Gong for XPS analysis and Prof. J.J. Gooding for access and assistance with electrochemical equipment.

### Supporting information

Crystallographic data for compound **3** have been deposited at the Cambridge Crystallographic Data Center (CCDC) under deposition number CCDC 759436. Copies can be obtained on request, free of charge, *via* www.ccdc.cam.ac.uk/conts/retrieving.html or from the Cambridge Crystallographic Data Centre, 12 Union Road, Cambridge CB2 1EZ, UK (fax: +44 1223-336-033 or email: deposit@ccdc.cam.ac.uk).

### REFERENCES

1. Bach U, Lupo D, Comte P, Moser JE, Weissortel F, Salbeck J, Spreitzer H and Grätzel M. *Nature* 1998; **395**: 583–585.

2. Ito S, Liska P, Comte P, Charvet R, Pechy P, Bach U, Schmidt-Mende L, Zakeeruddin SM, Kay A, Nazeeruddin MK and Grätzel M. *Chem. Commun.* 2005; 4351–4353.
3. Jayaweera PVV, Perera AGU and Tennakone K. *Inorg. Chim. Acta* 2008; **361**: 707–711.
4. Oregan B and Grätzel M. *Nature* 1991; **353**: 737–740.
5. Schmidt-Mende L, Bach U, Humphry-Baker R, Horiuchi T, Miura H, Ito S, Uchida S and Grätzel M. *Adv. Mat.* 2005; **17**: 813–815.
6. Yum J-H, Jung I, Baik C, Ko J, Nazeeruddin MK and Grätzel M. *Energy Environ. Sci.* 2009; **2**: 100–102.
7. Hicks JF, Miles DT and Murray RW. *J. Am. Chem. Soc.* 2002; **124**: 13322–13328.
8. Alvarez MM, Khoury JT, Schaaff TG, Shafiqullin MN, Vezmar I and Whetten RL. *J. Phys. Chem. B* 1997; **101**: 3706–3712.
9. Kesavan V, Sivanand PS, Chandrasekaran S, Kolytyn Y and Gedanken A. *Angew. Chem. Int. Ed.* 1999; **38**: 3521–3523.
10. Granot E, Patolsky F and Willner I. *J. Phys. Chem. B* 2004; **108**: 5875–5881.
11. Szulbinski W and Strojek JW. *Inorg. Chim. Acta* 1986; **118**: 91–97.
12. Kalyanasundaram K, Shelnutt JA and Grätzel M. *Inorg. Chem.* 1988; **27**: 2820–2825.
13. Kalyanasundaram K. *J. Photochem. Photobiol.* 1988; **42**: 87–109.
14. Fuhrhop J-H, Krüger W and David HH. *Liebigs. Ann. Chem.* 1982; 204–210.
15. Salker AV and Gokakakar SD. *Int. J. Phys. Sci.* 2009; **4**: 377–384.
16. Irie R, Li X and Saito Y. *J. Mol. Catal.* 1984; **23**: 17–22.
17. Silva E, Pereira MM, Burrows HD, Azenha ME, Sarrakha M and Bolte M. *Photochem. Photobiol. Sci.* 2004; **3**: 200–204.
18. Nazeeruddin MK, Humphry-Baker R, Officer DL, Campbell WM, Burrell AK and Grätzel M. *Langmuir* 2004; **20**: 6514–6517.
19. Wang Q, Campbell WM, Bonfantani EE, Jolley KW, Officer DL, Walsh PJ, Gordon K, Humphry-Baker R, Nazeeruddin MK and Grätzel M. *J. Phys. Chem. B* 2005; **109**: 15397–15409.
20. Campbell WM, Jolley KW, Wagner P, Wagner K, Walsh PJ, Gordon KC, Schmidt-Mende L, Nazeeruddin MK, Wang Q, Grätzel M and Officer DL. *J. Phys. Chem. C* 2007; **111**: 11760–11762.
21. Song Y, Yang Y, Medforth CJ, Pereira E, Singh AK, Xu H, Jiang Y, Brinker J, Van Swol F and Shelnutt JA. *J. Am. Chem. Soc.* 2004; **126**: 635–645.
22. Wang ZC, Medforth CJ and Shelnutt JA. *J. Am. Chem. Soc.* 2004; **126**: 16720–16721.
23. Chukharev V, Vuorinen T, Efimov A, Tkachenko NV, Kimura M, Fukuzumi S, Imahori H and Lemmetyinen H. *Langmuir* 2005; **21**: 6385–6391.
24. Hirano T, Yui T, Okazaki K-i, Kajino T, Fukushima Y, Inoue H, Torimoto T and Takagi K. *J. Nanosci. Nanotechnol.* 2009; **9**: 495–500.
25. McDonald AR, Franssen N, van Klink GPM and van Koten G. *J. Organomet. Chem.* 2009; **694**: 2153–2162.
26. Rothmund P and Menotti AR. *J. Am. Chem. Soc.* 1948; **70**: 1808–1812.
27. Brotherhood PR, Luck IJ, Blake IM, Jensen P, Turner P and Crossley MJ. *Chem-Eur. J.* 2008; **14**: 10967–10977.
28. Crossley MJ, Thordarson P and Wu RA-S. *J. Chem. Soc. Perkin Trans. 1* 2001; 2294–2302.
29. Huisgen R. *Proc. Chem. Soc.* 1961; 357–396.
30. Khoukhi N, Vaultier M and Carrié R. *Tetrahedron* 1987; **43**: 1811–1822.
31. Ortega-Munoz M, Lopez-Jaramillo J, Hernandez-Mateo F and Santoyo-Gonzalez F. *Adv. Synth. Catal.* 2006; **348**: 2410–2420.
32. Marrani AG, Dalchiele EA, Zanoni R, Decker F, Cattaruzza F, Bonifazi D and Prato M. *Electrochim. Acta* 2008; **53**: 3903–3909.
33. Ou Z, E W, Zhu W, Thordarson P, Sintic PJ, Crossley MJ and Kadish KM. *Inorg. Chem.* 2007; **46**: 10840–10849.
34. Szulbinski W, Zak J and Strojek JW. *J. Electroanal. Chem.* 1987; **226**: 157–170.
35. Wang Z, Lybarger LE, Wang W, Medforth CJ, Miller JE and Shelnutt JA. *Nanotechnology* 2008; **19**: 395604.
36. Kabschi W. *J. Appl. Cryst.* 1993; **26**: 795–800.
37. Sheldrick GM. *Acta Cryst. A* 2008; **64**: 112–122.
38. Osada T, Kugler T, Broms P and Salaneck WR. *Synth. Met.* 1998; **96**: 77–80.
39. Guo Z, Lei A, Liang X and Xu Q. *Chem. Comm.* 2006; 4512–4514.